Groundwater

Modeling Groundwater Inflow to the New Crater Lake at Kīlauea Volcano, Hawai'i

by S. E. Ingebritsen[1], A. F. Flinders[2], J. P. Kauahikaua[2], and P. A. Hsieh[3]

Abstract

During the 2018 eruption of Kīlauea Volcano, Hawai'i, scientists relied heavily on a conceptual model of explosive eruptions triggered when lava-lake levels drop below the water table. Numerical modeling of multiphase groundwater flow and heat transport revealed that, contrary to expectations, liquid water inflow to the drained magma conduit would likely be delayed by months to years, owing to the inability of liquid water to transit a zone of very hot rock. The summit of Kīlauea subsequently experienced an ~2-month period of consistent repeated collapses, and the crater now extends below the equilibrium position of the water table. Liquid water first emerged into the deepened crater in late July 2019. The timing of first appearance of liquid water (about 14 months postcollapse) and the rate of crater lake filling (currently ~27 kg/s) were well-predicted by the numerical modeling done in late spring 2018, which forecast liquid inflow after 3 to 24 months at rates of 10 to 100 kg/s. A second-generation groundwater model, reflecting the current crater geometry, forecasts lake filling over the next several years. The successful 2018 to present forecasts with both models are based on unadjusted in situ permeability estimates (1 to 6×10^{-14} m^2) and water-table elevations (600 to 800 m) from a nearby research drillhole and geophysical surveys. Important unknowns that affect the reliability of longer-term forecasts include the equilibrium water-table geometry, the rate of evaporation from the hot and growing crater lake (currently ~29,000 m^2 at 70-80 °C), and heterogenous permeability changes caused by the 2018 collapse.

Introduction

At least two fundamental hydrogeologic questions arose during and after the 2018 eruption of Kīlauea Volcano, Hawai'i. The first question was prompted by a classic conceptual model of explosive eruption at Kīlauea triggered by groundwater inflow to a recently vacated magma conduit (Figure 1), namely: How long would it take for liquid groundwater to reach the vacated conduit? Subsequently, a portion of the caldera floor collapsed below the expected position of the water table, prompting a second question: Would the deepened crater fill with water, and if so how fast, and to what level? Here we describe the successful prediction of system behavior to date and attempt to forecast crater-lake filling over the next several years. Essential differences between pre- and postcollapse hydrogeologic conditions prompted the choice of different groundwater models (HYDROTHERM and MODFLOW) and different system geometries to address the two motivating questions. However, both models adopt similar conceptualizations and data-constrained parameter values and yield similar early-time (2018 to present) predictions.

For 1500 of the past 2500 years, Kīlauea's eruptions were dominantly explosive, manifested by repeated phreatic and phreatomagmatic activity in a deep summit caldera (Swanson et al. 2014). The series of explosive eruptions ca. 1790 may have occurred when the caldera floor was below the water table (Mastin 1997). Thus, there will be persistent interest in the evolving crater lake and its relationship to the surrounding groundwater system and underlying magmatic system.

Pre- and Postcollapse HYDROTHERM Modeling of Groundwater Inflow

In early May 2018, the level of the lava lake on Kīlauea summit (Figure 2a) was dropping rapidly (~2 m/h; Neal et al. 2019). There was an expectation, based on observations and interpretations of the 1924 Kīlauea eruption, that groundwater inflow would trigger explosions when the lava lake dropped below the water table (Figure 1). On May 10, the Scientist-in-Charge at the Hawaiian Volcano Observatory requested model-based estimates of how long it would take for

[1]Corresponding author: U.S. Geological Survey, Moffett Field, California, U.S.A.; (650) 329 4422, fax: (650) 329 4463; seingebr@usgs.gov

[2]U.S. Geological Survey, Hilo, HI, CA

[3]U.S. Geological Survey, Menlo Park, CA

Article Impact Statement: Groundwater modeling elucidates the likelihood of explosions during the 2018 Kīlauea eruption and the ongoing growth of the new crater lake.

Received March 2020, accepted June 2020.

doi: 10.1111/gwat.13023

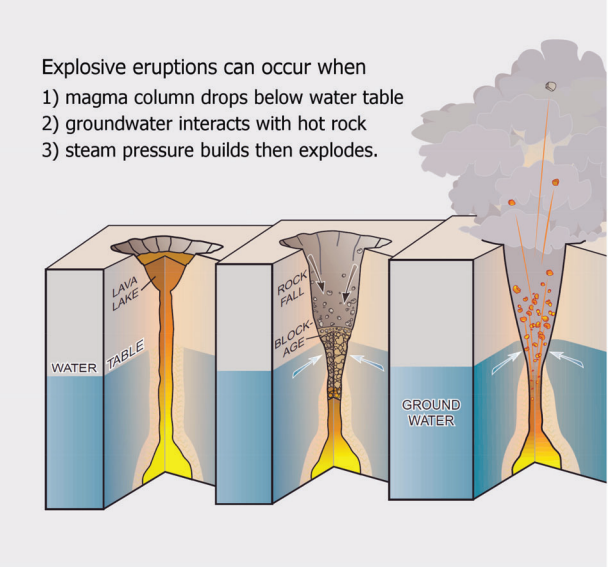

Figure 1. Conceptual model of 1924 Kīlauea explosions powered by steam generated as groundwater came in contact with hot rocks. Once the magma level drops below the water table, groundwater can flow into the still-hot conduit, where it quickly flashes to steam. This conceptual model owes mainly to Stearns (1925). Versions of this figure appear in Mastin et al. (1999) and Houghton et al. (2015), and were widely reproduced by the news media in early May 2018.

groundwater inflow to begin. Over approximately the next 72 h, a series of simulations were performed with the USGS HYDROTHERM model (https://volcanoes.usgs.gov/software/hydrotherm/) in order to address that question (Hsieh and Ingebritsen 2019). HYDROTHERM is one of the few documented, open-source codes that can handle magmatic temperatures (to 1200 °C) and multiphase flow—both of which were essential elements for addressing the problem at that time.

HYDROTHERM solves mass- and energy-balance equations that can be written as

$$\frac{\partial[\phi(S_l\rho_l + S_l\rho_l)]}{\partial t} - \nabla\cdot\left[\frac{\rho_l k_{rl}\bar{k}}{\mu_v}(\nabla P + \rho_l g\nabla z)\right] - \nabla\cdot\left[\frac{\rho_v k_{rv}\bar{k}}{\mu_v}(\nabla P + \rho_v g\nabla z)\right] - R_m = 0, \quad (1)$$

and

$$\frac{\partial[\phi(S_l\rho_l h_l + S_v\rho_v h_v) + (1-\phi)\rho_r h_r]}{\partial t} - \nabla\cdot\left[\frac{\rho_l k_{rl}\bar{k}h_l}{\mu_l}(\nabla P + \rho_l g\nabla z)\right] - \nabla\cdot\left[\frac{\rho_v k_{rv}\bar{k}h_v}{\mu_v}(\nabla P + \rho_v g\nabla z)\right] - \nabla\cdot K_m\nabla T - R_h = 0, \quad (2)$$

respectively. In order to allow for variations in fluid density (ρ) and viscosity (μ), these equations are posed

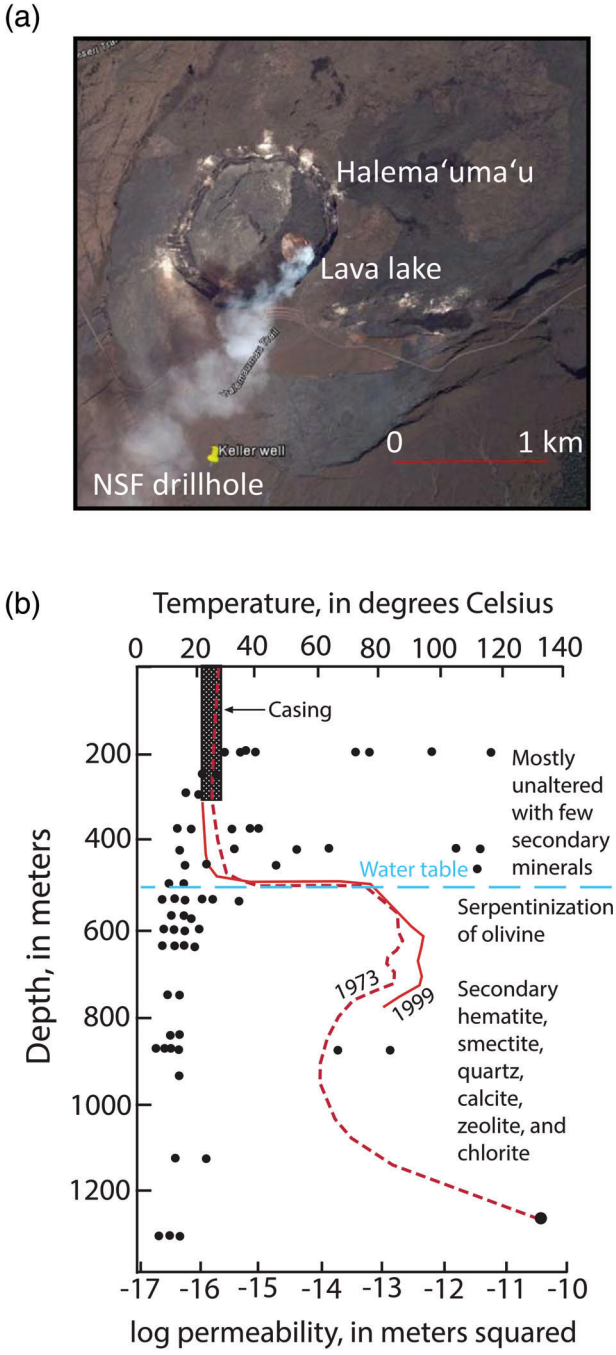

Figure 2. (a) Aerial photograph showing relative positions of Halema´uma´u, the lava lake, and the NSF drillhole ("Keller well") on Kīlauea summit prior to the 2018 eruption sequence and (b) temperature profiles (red lines), core-scale permeability measurements (black dots), water-table position (blue line), and brief description of hydrothermal alteration above and below the water table (Keller et al. 1979). Depths in (b) are relative to the derrick-floor elevation of 1102 m.

in terms of pressure (P) and elevation (z), rather than hydraulic head, and in terms of permeability (k), rather than hydraulic conductivity. Multiphase versions of Darcy's Law that include relative-permeability (k_r) terms are embedded in both the mass- and energy-balance equations, and the energy-balance equation (Equation 2)

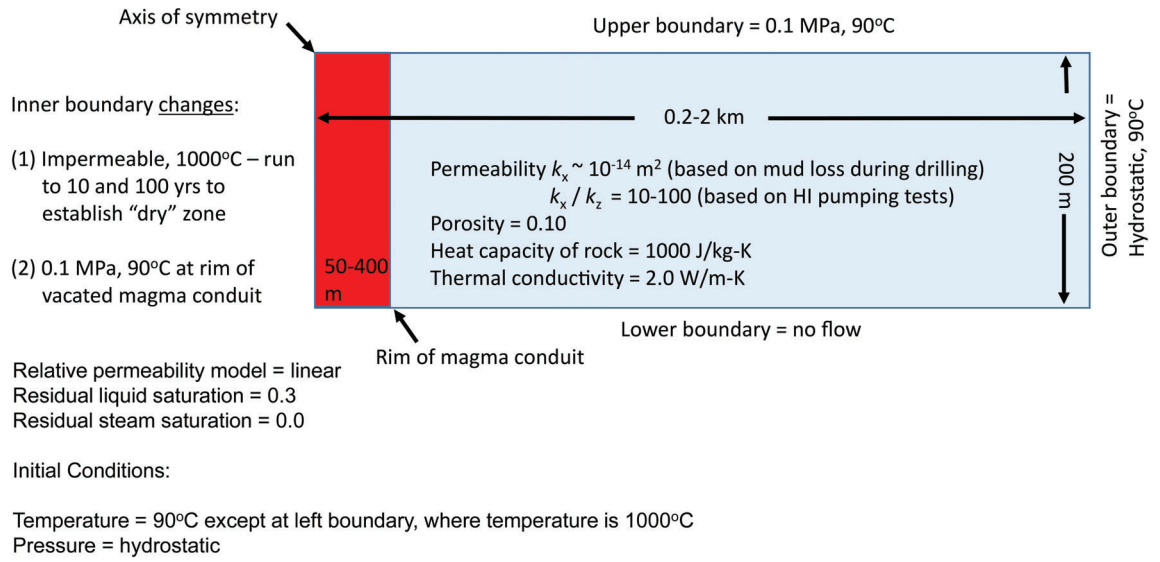

Figure 3. Geometry, boundary, and initial conditions, and key parameters for HYDROTHERM modeling of radial groundwater inflow towards a preheated volcanic conduit. The change in the inner (left-hand) boundary represents the (1) presence followed by (2) instantaneous drainage of a conduit filled with magma at 1000 °C. During stage (1) the inner boundary is closed to fluid flow but open to heat flow, and fluid pressures near the magma conduit are generally near hydrostatic, controlled by the upper- and outer-boundary pressures. During stage (2) the inner boundary is open to fluid flow, and fluid pressures near the vacated magma conduit are generally subhydrostatic. Relative permeabilities are invoked in multiphase flow simulations to represent the reduction in mobility of one fluid phase due to the interfering presence of other phases. They are treated as scalar functions of liquid volume saturation ($V_{\text{liquid}}/V_{\text{void}}$), and the linear function and residual saturation values invoked here are standard defaults for steam/liquid water flow (e.g., Ingebritsen et al. 2006).

is posed in terms of enthalpy (h), a convenient way of dealing with the latent heat of vaporization. The R terms represent source and sinks of fluid mass or heat, ϕ is porosity, S is volumetric saturation, g is gravitational acceleration, K_m is thermal conductivity of the medium, T is temperature, and the subscripts l, v, and r refer to liquid water, vapor (steam), and rock, respectively. The overline indicates that permeability is a second-rank tensor in the general case.

The HYDROTHERM model parameterization was based to a large extent on data from the only deep drillhole on Kīlauea summit, an NSF-funded drillhole about 1.5 south of the lava lake (Figure 2). Permeability is the single most important parameter governing potential inflow of groundwater. Murray (1974, 56 to 61) estimated the permeability of the 500 to 1200 m depth interval in the NSF drillhole to be 1×10^{-14} m^2 on the basis of rates of mud loss during drilling. He inferred a somewhat larger value of 6×10^{-14} m^2 from numerical-modeling experiments that simulated convection within a rectangular model and matched the distinctive temperature profile (Figure 2b). The mud-loss-based permeability value for the NSF drillhole (1×10^{-14} m^2) is an estimate of horizontal permeability, whereas the model-based value (6×10^{-14} m^2) assumes isotropic conditions. Both values are significantly larger than the permeability of core samples obtained in that interval ($\sim 5 \times 10^{-17}$ m^2; Figure 2b), but discrepancies of such magnitude ($\sim 10^3$) between core measurements and in situ-scale values are commonly observed in fractured crystalline rocks (Brace 1980, 247). The layering of lava flows introduces some anisotropy, and limited well-test data in Hawaiian lavas suggest vertical permeability (k_z) perhaps 10 to 200 times less than horizontal permeability (k_x) (Ingebritsen and Scholl 1993). Thus, the HYDROTHERM simulations considered k_x values of 10^{-13} to 10^{-14} m^2 and a range of anisotropies (k_x/k_x 10^1 to 10^2). In order to assess the possibility of rapid liquid-water inflow, it was deemed particularly important to explore the upper range of permeability values. Fluid pressures in the simulations were generally near-hydrostatic, because permeabilities on the order of $k_x = k_z \leq 10^{-17}$ m^2 are needed to maintain elevated pore-fluid pressures in geologic media (cf Neuzil 1995).

The flow system was modeled as a large, flat cylinder, with radial symmetry centered on the lava lake (Figure 3). The vertical dimension extended only from the water-table elevation in the NSF drillhole (~600 m elevation) to 200 m below the water table (~400 m elevation). Quantitative modeling of the distinctive temperature profile (Figure 2b) suggests lower permeability ($\sim \leq 10^{-16}$ m^2) below about 400 m elevation/700 m depth (Hurwitz et al. 2002). Thus, significant groundwater inflow was expected mainly within about 200 m of the water table. To represent drainage of the lava lake, the inner boundary of the HYDROTHERM model was instantaneously switched from (no-flow, 1000 °C) to (0.1 MPa, 90 °C) at a specified point in time.

The HYDOTHERM modeling (Hsieh and Ingebritsen 2019) revealed that the sustained presence of the lava lake (since March 2008: Orr et al. 2013) would have generated a cylinder of very hot rock around the underlying

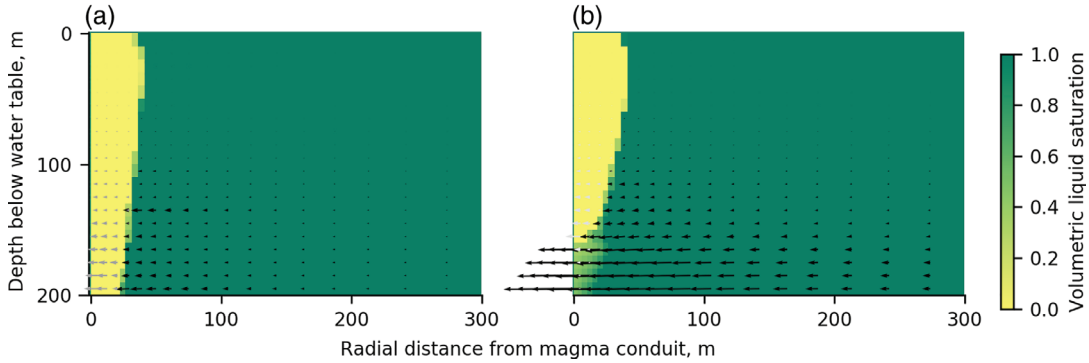

Figure 4. Liquid water saturation and flow vectors for liquid (black) and steam (gray) in host rock with $k_x = 10^{-14}$ m^2 and $k_x/k_z = 100$ (a) 1 year and (b) 3 years after drainage of a short-lived (10 years) and narrow (50 m radius) magma conduit. Rulers show distances in m. The enhanced flow at greater depths reflects the greater driving force for fluid flow after the inner boundary condition changes (after magma drainage, pressure along the inner boundary is held at 0.1 MPa—see Figure 3).

magma column. A steam zone (no mobile liquid water) develops around the magma conduit within 1 year and is ~30 m wide after 10 years. After the magma column falls below the water table (Figure 4), contrary to expectations, liquid water inflow to the drained conduit would likely be delayed by months to years (3 to 24 months), owing to the inability of liquid water to transit the surrounding zone of very hot rock. Immediate water vapor (steam) influx to the drained conduit, at rates on the order of 10 kg/s, seemed likely. However, water vapor at pressures of ~0.1 MPa expands only by a factor of ~4 when heated from 100 °C to 1000 °C and lacks the explosive potential of liquid water, which expands by a factor of roughly 10^3 upon converting to steam at near-atmospheric pressures.

Over an ~2-month period following the draining of the summit lava lake there was massive, progressive collapse of a portion of Kīlauea summit, such that the crater-floor elevation ultimately fell below the elevation of the water table in the NSF drillhole (Figure 5). This raised another hydrogeologic question: Would the crater fill with water (cf Mastin 1997), and if so how fast, and to what level?

A pond was first sighted in the deepened crater on July 26, 2019. Perhaps surprisingly, the preexisting HYDROTHERM model had accurately forecast both the timing (3 to 24 months) and early-time rate (10 to 100 kg/s) of liquid-water inflow (Figure 6). This successful forecast was unexpected for at least two reasons: the universal hydrogeologic issue of uncertainty with respect to permeability, and the fact that the new water lake is not exactly coincident with the former lava lake; rather, it is centered about ~200 m to the northwest (Figure 5). Further, the inner boundary condition—assumed constant in the model—was steadily changing, as lake level rose at a rate of about 1 m/week.

Postcollapse MODLOW Modeling of Groundwater Inflow

The good early-time forecasting ability of the HYDROTHERM model lent some confidence in the associated boundary conditions and parameter values (Figure 3). However, the caldera collapse essentially took a divot out of the large, flat cylinder modeled with HYDROTHERM (cf Figures 3 and 7), and gradual filling of the crater lake made the constant inner boundary condition of the HYDROTHERM model increasingly inappropriate over time.

A MODFLOW model (https://www.usgs.gov/mission-areas/water-resources/science/modflow-and-related-programs) was developed for the next stage of investigation, allowing flexible geometries and simulation of a moving water table. The thermal aspects of the problem now seemed secondary, and there was little evidence for multiphase flow in the depth range of interest. Adoption of MODFLOW also assumes that variable-density flow is not important at these relatively early times and shallow depths. The goals of the MODFLOW simulation were to see whether a simple groundwater-flow model could explain the observed water levels in the crater, and to forecast future water levels.

As a first approximation, the postcollapse crater (Figure 5, right panel) was approximated by an axisymmetric crater (Figure 7), with dimensions such that the volume of water in the simplified crater would be approximately the same as that in the actual crater. This conceptualization results in groundwater flowing radially toward the crater.

We further assume that, away from the crater, the water table is at an elevation of 600 m (the approximate water-table elevation in the NSF drillhole). As in the HYDROTHERM model, permeable rock is assumed to extend from 600 to 400 m elevation. The crater is represented as a porous medium with a high permeability and a porosity of 1, surrounded by rocks with properties similar to those used in the HYDROTHERM simulations. The model domain extends to an outer boundary at a distance of 1 km, at which distance the water table is assumed fixed at a constant elevation of 600 m.

Unlike HYDROTHERM (Equations 1 and 2), MODFLOW is formulated in terms of hydraulic head (h) and hydraulic conductivity (K). Hydraulic head (h) is related

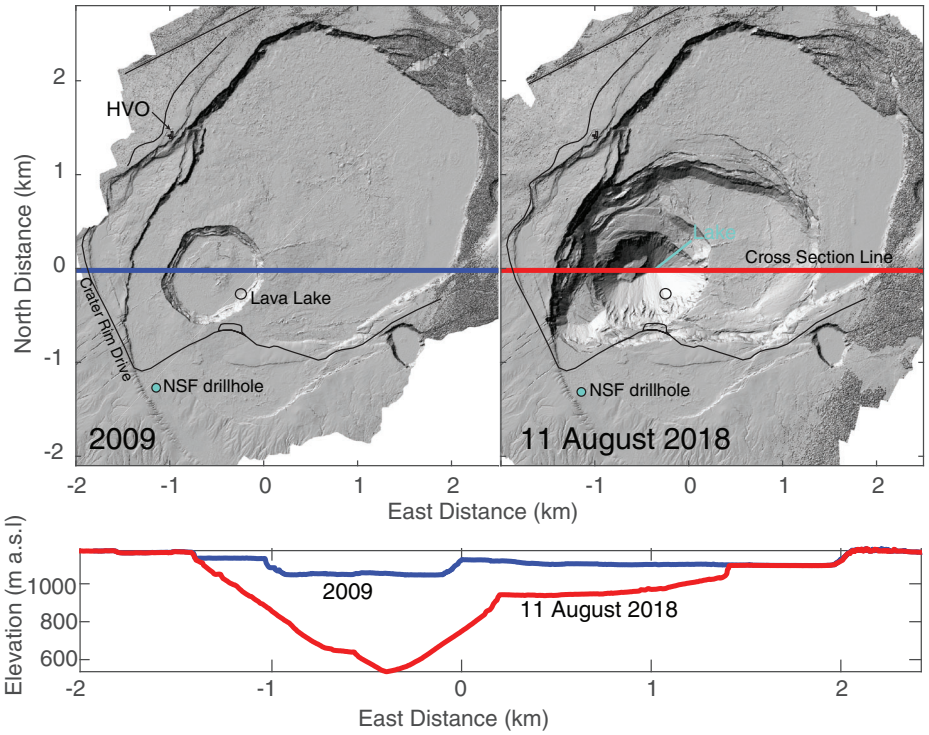

Figure 5. Caldera geometry pre- and postcollapse: LIDAR (light detection and ranging) digital elevation models of Kīlauea's summit from 2009 (left) and August 11, 2018 (right). Black lines indicate roads; the locations of the Hawaiian Volcano Observatory (HVO), former lava lake, and NSF research drillhole are indicated. The red and blue lines correspond to the locations of the cross sections shown in the lower panel. Following the collapse in mid-2018, crater depth extends below the elevation of the water table at the NSF drillhole (~600 m elevation). The growing water lake is NW of the former lava lake. After Neal et al. (2019).

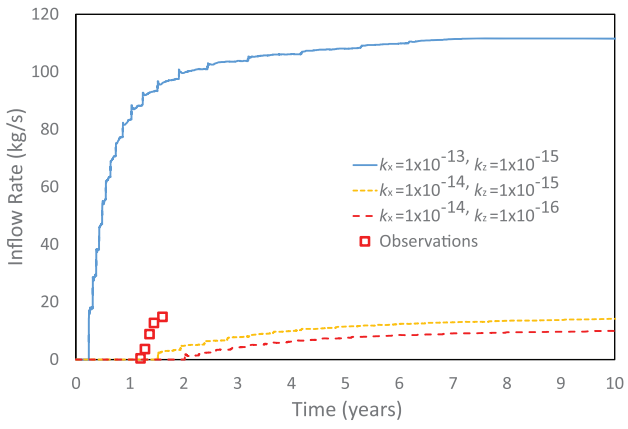

Figure 6. HYDROTHERM predictions of groundwater inflow to a recently vacated magmatic conduit for several combinations of horizontal (k_x) and vertical (k_z) permeability (Hsieh and Ingebritsen 2019) compared with early-time observations of the rate of crater lake filling. Lake volumes were estimated using the elevation of the lake surface, measured with a laser range finder, and a previously UAS collected digital elevation model (DEM). A second-order polynomial fit of the lake volume time-series was used to estimated flow rate. Here time = 0 is taken as mid-May 2018, the time at which the model predictions were made and prior to crater collapse (Figure 5).

to pressure (p) according to $h=p\rho g+z$, and hydraulic conductivity (K) is related to permeability (k) according to $K=\rho gk/\mu$. For the MODFLOW calculations, and for purposes of converting K values to k values, water properties are taken constant at 70 °C (the approximate water temperature both in the crater and near the water table in the NSF drillhole)—that is, $\rho = 978\,\text{kg/m}^3$ and $\mu = 0.0004\,\text{kg/m/s}$. The model ignores water input by precipitation, as well as water removal due to evaporation.

The MODFLOW simulations begin when the water table under the crater is just below the lowest point of the crater, that is, water is just about to emerge. The exact timing of this is not accurately known. The pond was first sighted on July 26, 2019, and the simulation begins on July 24, 2019. At this initial time, the elevation of the water table outside the crater is unknown. We expect the water table to have a shape that increases in elevation with increasing radial distance away from the crater, forming a "cone of depression" around the crater. To create this initial water table, we first make a steady state MODFLOW run in which the model cells inside the crater are removed, and the drain package is applied to cells at the crater surface. This model run yields a steady-state water table (Figure 7) that is used as the initial condition for the transient run.

The three values of permeability used for comparisons with observational data (Figure 8: $k_x = 3$, 4,

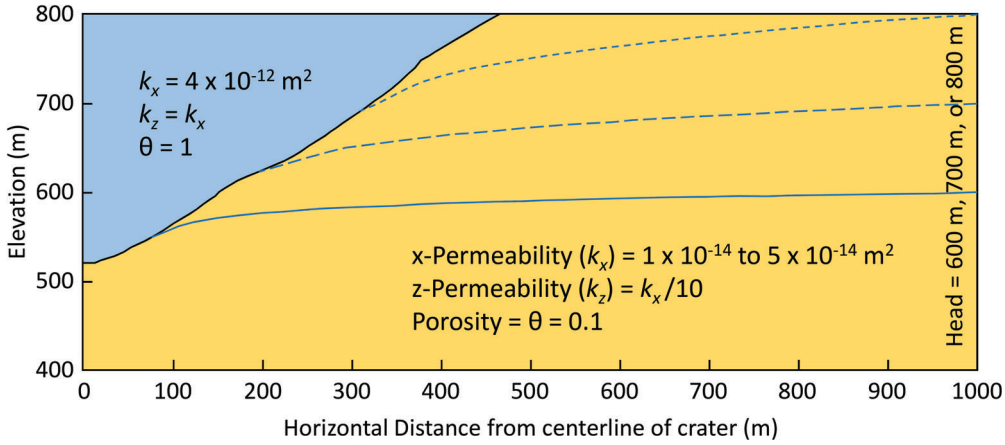

Figure 7. Schematic of postcollapse MODFLOW model. The new crater pit (light blue region) is simulated as a porous medium with high permeability and a porosity of 1. Blue lines indicate the initial positions of the water table: the solid blue line is for the case of equilibrium water table elevation at 600 m; the long-dashed line is for an equilibrium water table elevation at 700 m, and the short-dashed line is for an equilibrium water table elevation at 800 m.

and 5×10^{-14} m^2) are within the range of the NSF drillhole-based estimates of 1 to 6×10^{-14} m^2, and permeability anisotropies are similar to those invoked in the HYDROTHERM modeling ($k_x/k_z = 10$). Figure 8a shows the simulated crater lake volume superimposed on the measured volume (red dots), with the simulated curve for $k_x = 3 \times 10^{-14}$ m^2 closest to the measured data for $t < \sim$100 days. Figure 8b shows simulated rates of water inflow into the crater superimposed on measured inflow (gray line), and again the simulated curve for $k_x = 3 \times 10^{-14}$ m^2 is closest to the measured data for $t < \sim$100 days. The oscillations in the simulated water-inflow curves are due to instability in the model computational scheme, and could probably be reduced by using a finer grid and smaller time steps. The simulated curve for $k_x = 3 \times 10^{-14}$ m^2 suggests that the water inflow rate should peak around 100 days and then start to decline. However, there is no indication of a decline in the observational data.

Mindful of the fact that the simulated water inflow rate plateaued by ~100 days and was beginning to depart from observations (Figure 8b), we consider alternate scenarios in which the fixed head at the outer boundary is set at 700 and 800 m. This modification to the outer boundary condition would cause the lake to equilibrate at higher elevations and attain larger volumes (Figure 9). This alternative is motivated by the fact that pre-eruption geophysical observations (resistivity data) suggest the possibility of a higher water table at the crater lake location than at the NSF drillhole (Kauahikaua 1993). As the equilibrium water-table elevation increases, the permeabilities required to simulate comparable early-time inflow rates are slightly lower, but still within the range of the NSF drillhole-based estimates ($k_x = 1\text{-}2 \times 10^{-14}$ m^2 when the elevation of the equilibrium water table is at 800 m vs. $k_x = 3\text{-}5 \times 10^{-14}$ m^2 when the elevation of the equilibrium water table is at 600 m). With higher water-table elevations, the simulated lake volumes are larger at later times (Figure 9a) and the inflow rate levels off considerably later (Figure 9b; ~1 year for an 800-m water table vs. ~100 days for a 600-m water table).

The MODFLOW simulations demonstrate that a simple model of groundwater flow, using reasonable values of permeability, can yield simulated crater-lake levels and volumes that are close to those observed. As additional data are collected, further comparisons between observations and model simulations may improve understanding of the groundwater flow system in the volcano. This will be a persistent topic of interest because, for 1500 of the past 2500 years, Kīlauea eruptions were manifested by repeated phreatic and phreatomagmatic activity in a deep summit caldera (Swanson et al. 2014).

Sources of Uncertainty in Longer-Term Forecasts

A number of factors that are either unknown and/or neglected in the modeling lend uncertainty to the longer-term forecasts and warrant further investigation. These include the water-table configuration, permeability structure, and lake evaporation rates.

We assumed radial symmetry in both the HYDROTHERM and MODFLOW models (Figures 3 and 7), with a constant water-table elevation at the outer boundary. However, in the general case, we expect both lateral flow owing to regional head gradients and evolving, likely asymmetrical water-table responses to the 2018 collapse. At Kīlauea summit, groundwater flow is generally southward toward the coastline from the higher, wetter north side of the caldera (e.g., Scholl et al. 1996). Regional groundwater gradients would cause asymmetrical heating, cooling, and throughflow that cannot be represented in cylindrical coordinates. Furthermore, the pre-eruption electrical conductor described by Kauahikaua (1993), and proposed to represent the water table, actually exhibited considerable relief. Based on

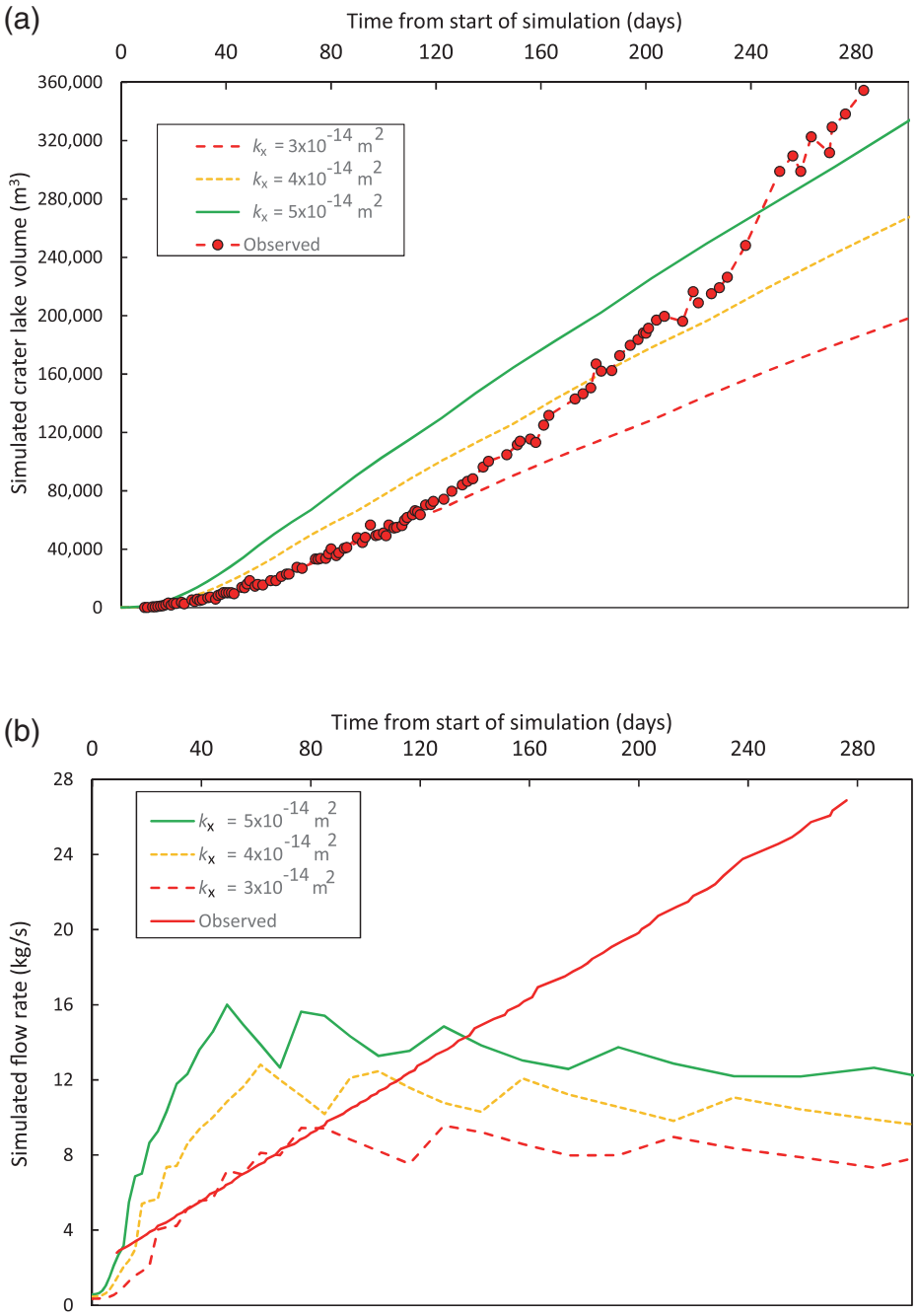

Figure 8. MODFLOW predictions of groundwater inflow to the emerging crater lake for several values of k_x and $k_x/k_z = 10$ compared with observations of the rate of lake filling: (a) simulated lake volume (solid and dashed lines) superimposed over graph of measured lake volume (red dots) and (b) simulated water flow rate into crater pit superimposed over observed filling rate (red line), with oscillations due to slight numerical instability in the model. Here time = 0 is taken as the first observation of standing water in the deepened crater (late July 2019).

those data, the pre-eruption water-table elevation near the growing crater lake may have been greater than 100 m higher than that observed at the NSF drillhole. Future geophysical surveys may help to map an evolving, and likely asymmetric, water-table configuration.

We also assumed uniform permeabilities consistent with the in situ-scale permeability estimates from the NSF drillhole. Permeability in general is an extremely heterogenous property (e.g., Gleeson and Ingebritsen 2017), varying in both space and time to the extent that it sometimes seems to defy systematic characterization. Further, the caldera collapse (Figure 5) seems likely to have influenced permeability in the vicinity of the crater lake. Thus, it is perhaps surprising that simple models using unadjusted data from a single observation point have provided good forecasts. However, in light of the results to date (Figures 6, 8, 9) there is as yet little motivation to invoke more complex permeability structures.

Finally, we neglected evaporation from the growing crater lake (Figure 10), which is likely an increasingly

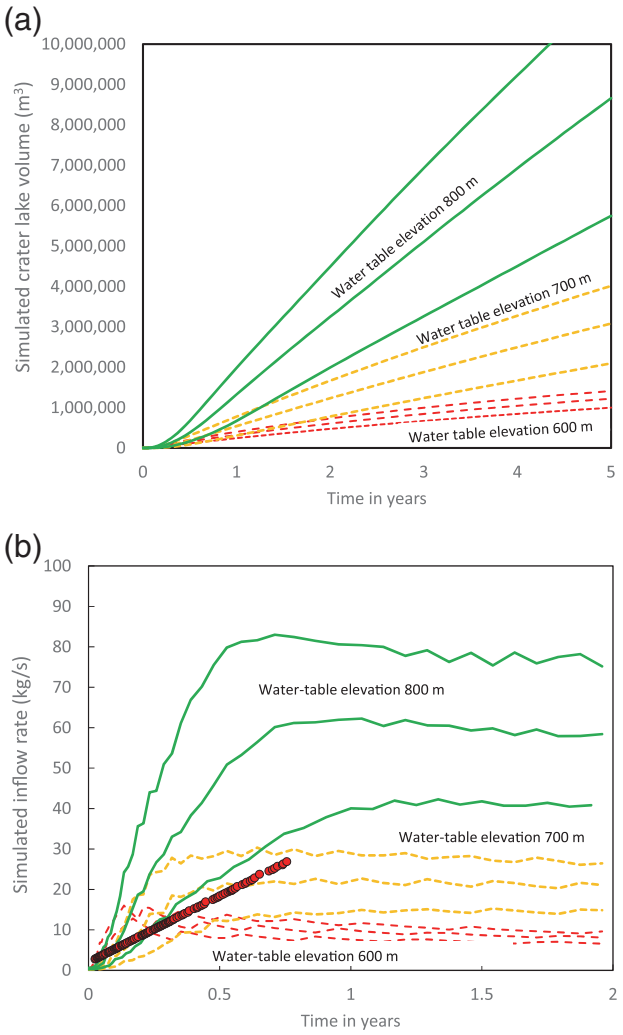

Figure 9. (a) MODFLOW forecast of crater lake volume projected to 5 years' time for several equilibrium water-table elevations. For a water-table elevation of 600 m, k_x ranges from 3 to 5 × 10^{-14} m^2; for water-table elevations of 700 and 800 m, k_x ranges from 1 to 2 × 10^{-14} m^2; and all simulations invoke $k_x/k_z = 10$. (b) MODFLOW-simulated water flow rate into crater pit projected to 2 years' time for the same water-table elevations and permeabilities as in (a); red dots represent observations to date. In both (a) and (b), the uppermost curve in each line triplet corresponds to the highest permeability, and time = 0 is taken as the first observation of standing water in the deepened crater (late July 2019).

important factor. The evaporation rate from Boiling Springs Lake at Lassen, California, smaller (13,000 m^2) and somewhat cooler (50 °C) than the Kīlauea crater lake as of this writing (~29,000 m^2 and 70-80 °C; Sara Peek, U.S. Geological Survey, written communication, 2020), was estimated as ~15 kg/s in the late 1980s (Sorey and Colvard 1994). Measurements of heat loss at the Obsidian Pool Thermal Area, Yellowstone, inferred even larger area-normalized evaporation rates from somewhat hotter (48-81 °C) water surfaces (Hurwitz et al. 2012). The evaporation rate at Kīlauea may be similar to these other examples, proportional to lake surface area, and increasing with time. As of this writing it may thus be

Figure 10. Photo of the 22-m-deep crater lake as of January 2, 2020; lateral dimensions 190 × 85 m, surface temperature 70 to 80 °C.

similar in magnitude to the simulated inflow rates in the HYDROTHERM (Figure 6) and MODFLOW (Figure 8b) models and to the current lake-filling rate (Figure 8b, red line). Evaporation at such rates would imply that the actual lake inflow rate is substantially larger than the lake-filling rate (currently ~27 kg/s). Even so, it would still be within the broad range of 10 to 100 kg/s predicted by the HYDROTHERM and MODFLOW models using unadjusted permeability values from the NSF drillhole. Future modeling studies should refine evaporation-rate estimates and treat evaporation as the significant sink that it has likely become.

Summary

For 1500 of the past 2500 years, Kīlauea's eruptions were dominantly explosive and associated with a deep summit caldera (Swanson et al. 2014). Thus, the current caldera configuration (Figure 5, right panel) will inspire persistent interest in the evolving hydrogeologic conditions. To this point in time, simple, radially symmetrical HYDROTHERM (Figure 3) and MODFLOW (Figure 7) models that invoke uniform and unadjusted parameters have led to accurate forecasts of the timing and rate of liquid water inflow (Figures 6 and 9b). They provide a framework for future models that could explore more complex water-table configurations and permeability structures and include evaporation from the growing crater lake as an important sink.

The groundwater modeling effort to date is consistent with the recent U.S. National Academy of Sciences recommendation to use physically based modeling in order to supplement traditional volcano-forecasting approaches, which rely mainly on pattern recognition in monitoring data and the geologic record (National Academy of Sciences 2017). This example shows how simplified

numerical models can be usefully applied to complex systems, despite the high level of uncertainty around physical parameters, especially permeability. Comparison between the numerical results and physical observations demonstrates how this type of modeling can be used to predict groundwater flow during complex, developing situations. This is important because volcanoes with active groundwater systems are prone to hazardous phreatic and phreatomagmatic explosions during eruptions and at times of change.

Acknowledgments

This work was supported by the USGS Volcano Hazards Program. The modeling software, documentation, and sample input files are available at https://volcanoes.usgs.gov/software/hydrotherm/. We declare no conflict of interest, and thank Frances Boreham (University of Bristol), Hedeff Essaid (U.S. Geological Survey), and Grant Ferguson (University of Saskatchewan) for helpful advice on previous versions of this paper and Matt Patrick, Katie Mulliken, and Don Swanson for crater-lake measurements. Angie Diefenbach and Michael Zoeller provided the digital elevation model used to calculate crater-lake volume. William Tollett implemented crater-lake values into the accessed database. Any use of trade, firm, or product names is for descriptive purposes only and does not imply endorsement by the U.S. Government.

Authors' Note

The authors do not have any conflicts of interest or financial disclosures to report.

References

Brace, W.F. 1980. Permeability of crystalline and argillaceous rocks. *International Journal of Rock Mechanics and Mining Science and Geomechanics Abstracts* 17, no. 5: 241–251.

Gleeson, T., and S.E. Ingebritsen (Eds). 2017. *Crustal Permeability*, 451. AGU/Wiley Blackwell: Chichester.

Houghton, B., J.D.L. White, and A.R. Van Eaton. 2015. Phreatomagmatic and related eruption styles. In *Chapter 30:* Encyclopedia of Volcanoes, 2nd ed., ed. H. Sigurdsson, 537–552. London: Academic Press.

Hsieh, P.A., and S.E. Ingebritsen. 2019. Groundwater inflow toward a preheated volcanic conduit: Application to the 2018 eruption at Kilauea volcano, Hawai'i. *Journal of Geophysical Research* 124, no. 2: 1498–1506. https://doi.org/10.1029/2018JB017133

Hurwitz, S., R.N. Harris, C.A. Werner, and F. Murphy. 2012. Heat flow in vapor dominated areas of the Yellowstone Plateau Volcanic Field: Implications for the thermal budget of the Yellowstone Caldera. *Journal of Geophysical Research* 117, no. B10. https://doi.org/10.1029/2012JB009463

Hurwitz, S., S.E. Ingebritsen, and M.L. Sorey. 2002. Episodic thermal perturbations associated with groundwater flow: An example from Kilauea Volcano, Hawaii. *Journal of Geophysical Research* 107, no. B11. https://doi.org/10.1029/2001JB001654

Ingebritsen, S.E., W.E. Sanford, and C.E. Neuzil. 2006. *Groundwater in Geologic Processes*, 2nd ed., 536. Cambridge University Press: Cambridge.

Ingebritsen, S.E., and M.A. Scholl. 1993. The hydrogeology of Kilauea volcano. *Geothermics* 22, no. 4: 255–270.

Kauahikaua, J.P. 1993. Geophysical characteristics of the hydrothermal systems of Kilauea Volcano, Hawai'i. *Geothermics* 22, no. 4: 271–299.

Keller, G.V., L.T. Grose, J.C. Murray, and C.K. Skokan. 1979. Results of an experimental drill hole at the summit of Kilauea Volcano, Hawaii. *Journal of Volcanology and Geothermal Research* 5, no. 3–4: 345–385.

Mastin, L.G. 1997. Evidence for water influx from a caldera lake during the explosive hydromagmatic eruption of 1790, Kīlauea volcano, Hawai'i. *Journal of Geophysical Research* 102, no. B9: 20,093–20,109.

Mastin, L.G., R.L. Christiansen, D.A. Swanson, P.H. Stauffer, and J.W. Hendley. 1999. Explosive eruptions at Kilauea Volcano, Hawaii? *U.S. Geological Survey Fact Sheet*: 132–98. Reston, Virginia: USGS.

Murray, J.C. 1974. The geothermal system at Kilauea Volcano, Hawaii. Ph.D. thesis, Colorado School of Mines, Golden, Colorado.

National Academy of Sciences Committee on Improving Understanding of Volcanic Eruptions. 2017. *Volcanic Eruptions and their Repose, Unrest, Precursors, and Timing*, 122. Washington, DC: The National Academies Press http://nap.edu/24650

Neal, C.A., S.R. Brantley, L. Antolik, J.L. Babb, M. Burgess, K. Calles, M. Cappos, J.C. Chang, S. Conway, L. Desmither, P. Dotray, T. Elias, P. Fukunaga, S. Fuke, I.A. Johanson, K. Kamibayashi, J. Kauahikaua, R.L. Lee, S. Pekalib, A. Miklius, W. Million, C.J. Moniz, P.A. Nadeau, P. Okubo, C. Parcheta, M.R. Patrick, B. Shiro, D.A. Swanson, W. Tollett, F. Trusdell, E.F. Younger, M.H. Zoeller, E.K. Montgomery-Brown, K.R. Anderson, M.P. Poland, J.L. Ball, J. Bard, M. Coombs, H.R. Dietterich, C. Kern, W.A. Thelen, P.F. Cervelli, T. Orr, B.F. Houghton, C. Gansecki, R. Hazlett, P. Lundgren, A.K. Diefenbach, A.H. Lerner, G. Waite, P. Kelly, L. Clor, C. Werner, K. Mulliken, G. Fisher, and D. Damby. 2019. The 2018 rift eruption and summit collapse of Kīlauea Volcano. *Science* 363, no. 6425: 367–374.

Neuzil, C.E. 1995. Abnormal pressures as hydrodynamic phenomena. *American Journal of Science* 295: 742–786.

Orr, T.R., W.A. Thelen, M.R. Patrick, D.A. Swanson, and D.C. Wilson. 2013. Explosive eruptions triggered by rockfalls at Kīlauea volcano, Hawai'i. *Geology* 41, no. 2: 207–210. https://doi.org/10.1130/G33564.1

Scholl, M.A., S.E. Ingebritsen, C.J. Janik, and J.P. Kauahikaua. 1996. Use of precipitation and groundwater isotopes to interpret regional hydrology on a tropical volcanic Island: Kilauea volcano area, Hawaii. *Water Resources Research* 32, no. 12: 3525–3537.

Sorey, M.L., and E.M. Colvard. 1994. Measurements of heat and mass flow from thermal areas in Lassen Volcanic National Park, California, 1984-93. *U.S. Geological Survey Water-Resources Investigations Report* 94-4180-A. Reston, Virginia: USGS.

Stearns, H.T. 1925. The explosive phase of Kilauea Volcano, Hawaii, in 1924. *Bulletin Volcanologique* 2, no. 2: 194–208. https://doi.org/10.1007/BF02719505

Swanson, D.A., T.R. Rose, A.E. Mucek, M.O. Garcia, R.S. Fiske, and L.G. Mastin. 2014. Cycles of explosive and effusive eruptions at Kīlauea Volcano, Hawai'i. *Geology* 42, no. 7: 631–634.